

Automated Crystal Orientation Mapping (ACOM) with a Computer-Controlled TEM by Interpreting Transmission Kikuchi Patterns

R.A. Schwarzer and J. Sukkau

Institut für Metallkunde und Metallphysik der TU, D-38678 Clausthal-Z., Germany

Keywords: BKD, TKD, TEM, Pattern Recognition, Image Processing, Aggregate Function, Electron Diffraction

Abstract

A system for acquisition and interpretation of transmission Kikuchi patterns with a computer-controlled PHILIPS EM 430 TEM is presented. It enables interactive as well as fully automated determination of individual grain orientations using digital beam scan for ACOM operation. A high-grade integrating CCD camera is mounted on-axis on the bottom flange of the microscope column. Image resolution is 1,024 by 1,024 pixels, the dynamic range is 14 bit. With the present setup more than 3,000 orientations can be measured unattendedly per hour.

1. Introduction

Modern electron diffraction methods enable local texture and point-to-point orientation correlations to be determined routinely [1]. *Automated Crystal Orientation Measurement/Mapping* (ACOM) with digital beam scan in particular has evolved as a convenient alternative to x-ray pole figure measurement since it allows a fast study of selected small areas of any shape and the construction of the complete ODF without suffering from ghost problems or inconsistent x-ray diffraction data which have to be acquired at varying angles of specimen tilt. *Backscatter Kikuchi Diffraction* (BKD) as the most common technique, however, is limited to materials with grain sizes exceeding at least a tenth of a micron, low to medium local strain, high electrical conductivity and a rather plane surface which has to be free from foreign layers. *Transmission Kikuchi Diffraction* (TKD) is not subject to these limitations. With a medium voltage TEM the cumbersome preparation of transparent samples is much alleviated because beam penetration is in the micron range in Kikuchi diffraction. Hence an extremely large number of grains, indeed, can often be studied in one fine-grain specimen.

Transmission Kikuchi patterns require a different approach for automated interpretation concerning hard as well as software as compared to the more common backscatter Kikuchi patterns in the SEM. This is due to the extremely steep increase of background close to the pattern center (primary beam spot), the presence of interfering diffraction spots, the presence of (bright) excess and (dark) defect Kikuchi lines and a specific distribution of intensity across the bands.

2. Experimental setup for individual grain orientation measurement in the TEM

A high-grade charge-coupled device (CCD) camera GATAN type 794 10BP.4 has been mounted on-axis on the bottom flange of the projection chamber housing of our Philips EM 430 TEM. The camera is fiber-optically coupled to a phosphor screen and cooled by a Peltier cooler. The CCD sensor consists of 1,024 · 1,024 pixels, each pixel is 24 μm · 24 μm wide.

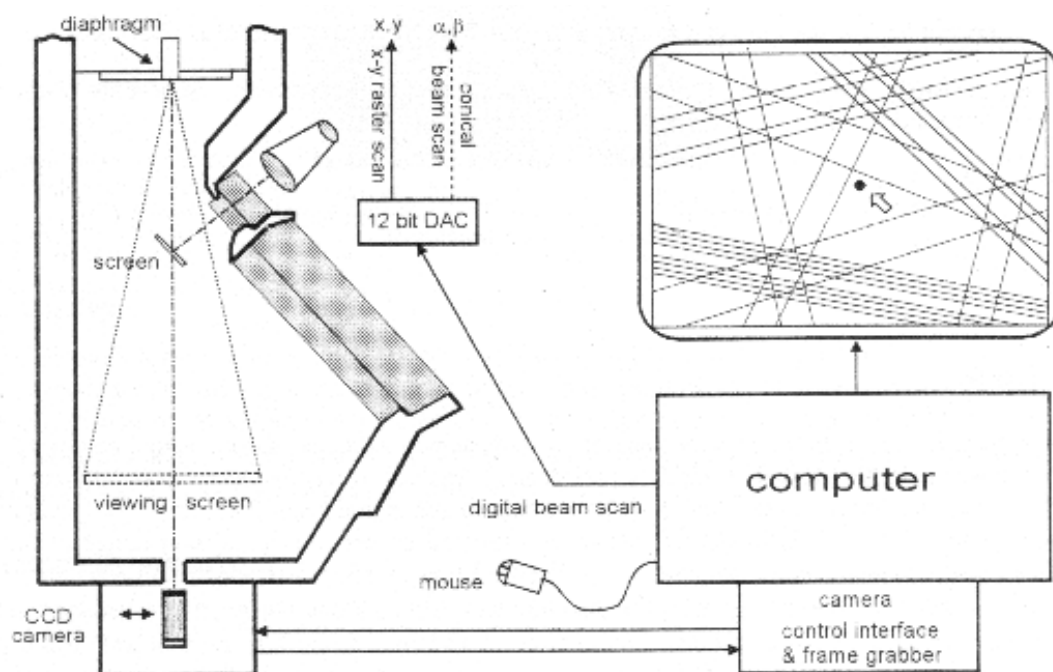


Figure 1 Set-up for the automated crystal lattice orientation mapping (ACOM) and interactive grain orientation measurement with a PHILIPS EM 430 TEM.

Figure 1 shows a schematic drawing of the setup. In order to accept a wide angular range of a transmission Kikuchi pattern on the camera chip, the camera length of the microscope has been reduced to 65 mm by changing the EPROM program of the lens control hardware. The video image is digitized and transferred to the computer with a resolution of 14 bit which corresponds to 16,384 gray levels. In order to speed up read-out at reduced resolution, x2, x3, x4 and x8 binning as well as 8 bit digitization are supported as software-controlled options. A digital beam control of 12 bit resolution (4,096 by 4,096 image points) has been developed to position the primary beam spot on a regular grid in a polygon-shaped area, along a line or on selected points by the computer program. The system is Pentium PC based on the MS-Windows[®] 95/NT platform.

3. Interactive determination of grain orientations

For the interactive on-line measurement selected features to be measured are marked with the mouse in the diffraction pattern on the monitor screen (first the primary beam spot representing the reference direction of the beam, then (diffraction spots or) points on the center line of a Kikuchi band or points on the Kikuchi lines bordering a band, respectively). The same technique can be used for measuring geometrical features such as dislocation lines, slip lines, stacking faults, extinction contours or grain boundaries in the microstructure image by simply

switching the microscope to imaging mode of operation [2]. The program makes allowance for image rotation as a function of mode of operation, accelerating voltage, camera length and magnification. As a cheap alternative for the CCD camera, the read-out of selected x-y positions in the diffraction patterns or images by using the built-in deflection coils of the TEM [3] is still available.

The geometry of the patterns is unique for a particular crystal structure and crystal lattice orientation. Indexing is based on the comparison of measured interplanar angles and interplanar spacings with theoretical values calculated for the actual crystal structure [4]. If only the center lines of Kikuchi bands have been measured, the program checks for interplanar angles *which correspond to the angles between the Kikuchi bands ("center line method")*. This method is particularly fast and adequate for cubic, tetragonal and hexagonal crystal symmetries. With lower crystal symmetry the reciprocal space becomes increasingly more populated and the number of possible interplanar angles increases. Then indexing is more reliable if interplanar spacings are considered as well. For this end the Kikuchi lines bordering the bands rather than the center lines have to be measured since the band widths are proportional to twice the Bragg angle. It is sufficient to evaluate the ratios of the band widths (*"ratio method"* as a program option) since all Kikuchi bands (or diffraction spots) of one pattern have been formed at the same accelerating voltage or wavelength, λ , and camera length, L . Hence the diffraction length, $\lambda \cdot L$, as a common scaling factor is skipped from calculation by considering the ratios of band widths (or of spacings from the primary beam spot to the diffraction spots, respectively). Only rough estimates of the accelerating voltage and the camera length are required to correct for the gnomonic projection of the pattern on the flat screen. If the accelerating voltage and the camera length are exactly known, however, indexing is performed faster by directly checking the interplanar angles *and* Bragg angles with their theoretical values (*"absolute method"* as another program option).

The crystal symmetries of the Laue group are supported. The calculations of interplanar angles and spacings are performed for all crystal symmetries by transforming the reciprocal lattice vectors, $\mathbf{g}(hkl)$, into an orthonormal coordinate system, $\mathbf{g}^o(hkl)$, by matrix multiplication with the inverse crystal matrix, \mathbf{A}^{-1} :

$$\mathbf{g}^o(hkl) = \mathbf{g}(hkl) \cdot \mathbf{A}^{-1} \quad (1)$$

with the crystal matrix \mathbf{A} :

$$\mathbf{A} = \begin{pmatrix} a & b \cdot \cos \gamma & & c \cdot \cos \beta \\ 0 & b \cdot \sin \gamma & & c \cdot (\cos \alpha - \cos \beta \cdot \cos \gamma) / \sin \gamma \\ 0 & 0 & c \cdot [1 + 2 \cdot \cos \alpha \cdot \cos \beta \cdot \cos \gamma - (\cos^2 \alpha + \cos^2 \beta + \cos^2 \gamma)]^{1/2} / \sin \gamma & \end{pmatrix}$$

$a, b, c, \alpha, \beta, \gamma$ denote the crystal parameters of the unit cell [5].

The calculation of interplanar angles, $\angle[\mathbf{g}(hkl)_i, \mathbf{g}(hkl)_j]$, and spacings, d_{hkl} , is thus reduced in orthonormalized space to:

$$\angle[\mathbf{g}(hkl)_i, \mathbf{g}(hkl)_j] = \arccos [(\mathbf{g}^o(hkl)_i \cdot \mathbf{g}^o(hkl)_j) / (|\mathbf{g}^o(hkl)_i| \cdot |\mathbf{g}^o(hkl)_j|)] \quad (2)$$

$$1/d_{hkl} = \sqrt{\mathbf{g}^o(hkl) \cdot \mathbf{g}^o(hkl)} \quad (3)$$

Transformation (1), angular (2) and spacings calculation (3) are carried out only once for a crystal structure and then stored in the computer memory in the form of look-up tables.

Indexing is performed by sorting out consistent sets of (hkl) whose theoretical interplanar spacings, d_{hkl} , and interplanar angles, $\angle[\mathbf{g}(\text{hkl})_i, \mathbf{g}(\text{hkl})_j]$, are in accord, within given tolerance with the values of the measured bands. The angles $\angle[\mathbf{n}(\text{hkl})_i, \mathbf{r}]_{\text{exp}}$ between a reference direction \mathbf{r} and the band normals $\mathbf{n}(\text{hkl})_i$ are known from the diffraction geometry and the band coordinates in the pattern. The spatial orientation of the diffraction vectors $\mathbf{g}(\text{hkl})_i$ (i.e. lattice plane normals) related to the bands $(\text{hkl})_i$ follow by considering the inclinations of the lattice planes to the primary beam direction simply by measuring the distances between the corresponding bands and the primary beam spot. Hence the angles $\angle[\mathbf{g}(\text{hkl})_i, \mathbf{r}]_{\text{exp}}$ between a reference direction \mathbf{r} and the diffraction vectors $\mathbf{g}(\text{hkl})_i$ are known as well, and the directional indices [uvw] of any reference direction \mathbf{r} can be calculated by solving the set of equations:

$$\begin{aligned} \mathbf{g}(\text{hkl})_i \cdot \mathbf{r} &= h_i u + k_i v + l_i w = \cos(\angle[\mathbf{g}(\text{hkl})_i, \mathbf{r}]_{\text{exp}}) \\ \mathbf{g}(\text{hkl})_j \cdot \mathbf{r} &= h_j u + k_j v + l_j w = \cos(\angle[\mathbf{g}(\text{hkl})_j, \mathbf{r}]_{\text{exp}}) \\ &\dots \\ \mathbf{g}(\text{hkl})_k \cdot \mathbf{r} &= h_k u + k_k v + l_k w = \cos(\angle[\mathbf{g}(\text{hkl})_k, \mathbf{r}]_{\text{exp}}) \\ &|\mathbf{r}| = 1 \end{aligned} \quad (4)$$

Since a reciprocal lattice vector, $\mathbf{g}(\text{hkl})_i$, is multiplied with a vector in real space, \mathbf{r} , these equations are valid for all crystal symmetries. At least two linearly independent Kikuchi bands i and j (or two non-collinear spots), have to be measured, but in this case the solution is ambiguous by a 180° rotation about the zone axis. A unique solution is only possible from at least three Kikuchi bands i , j and k which do not have a zone axis in common (or from three or more diffraction spots of different zones). For more than three linearly independent bands i , j , ..., k a best fit of all consistent solutions is taken. Details of the routines for indexing and orientation calculation can be found in [6]. In order to remove the 180° ambiguity by visual inspection, the program enables the rotation of the calculated orientation about three independent axes, a feature which simulates the tilt of the sample in the microscope stage. Rotation is carried out on the computer until a distinctly different pattern is shown on the screen. The specimen is then tilted about the same angles in the microscope. If the initial orientation was correct, the pattern on the microscope screen matches with that one on the computer monitor.

After orientation calculation has been completed, the recalculated pattern is displayed on the computer monitor for comparison with the measured pattern. The operator can switch between a Kikuchi or spot pattern on the monitor screen by a key stroke. He decides, whether the solution is correct and, if not, proceeds with indexing until the correct solution is found. The result can be stored on a file in (hkl)[uvw] notation, in the form of the \mathbf{g} orientation matrix or Euler angles, optionally along with further acquisition parameters such as a running number, and x-y coordinates.

4. The fully automated measurement and interpretation of Kikuchi patterns

Orientation measurement is often the start-off point of a detailed inspection and analysis of the microstructure such as Burgers vector analysis or the determination of glide systems [2]. Then the interactive measurement of Kikuchi band positions at a single grain of interest is adequate. In texture analysis, however, interactive measurement is now replaced by automated acquisition and indexing as the more convenient technique. For indexing Kikuchi patterns it is sufficient to know the positions rather than the accurate intensities of Kikuchi bands. The pattern is displayed in a window on the computer monitor. The operator has simply to direct, in imaging mode of operation, the focused primary beam on the grain of interest, and switch to diffraction mode. By a key stroke the pattern is captured and indexed without further interaction. Finally the operator compares the overlay image of the measured with the simulated Kikuchi pattern for correctness.

The automated extraction of band positions from the digitized Kikuchi pattern is more difficult in the TEM than in the SEM since background of a TKP is very intense and varies considerably across the pattern, intense diffraction spots frequently superimpose the Kikuchi pattern, particularly at sites where the sample is thin, and sharp bright and dark Kikuchi lines as well as bright Kikuchi bands have to be considered rather than bright bands only in the SEM. Normalization on a flat image cannot remove more than some artifacts from the screen (or the YAG glass) and the CCD chip, whereas background intensity strongly depends on the specific Kikuchi pattern, i.e. the actual grain orientation reflected by the arrangement of bands, and local foil thickness. In an earlier approach [4] background has been modeled with analytical fitting functions after having cut off excessive peak intensities from diffraction spots. A superior approach, however, is the calculation of a flat image, B, from each diffraction pattern, A, by a fast consolidation-expansion procedure of the digitized pattern A, followed by normalization A/B which also removes background intensity as well as diffraction spots, and a Laplace filter in order to enhance the Kikuchi band edges on the flattened background (Fig. 2). Radon transforms $R(\rho, \varepsilon)$ are finally applied to the digital gray-tone pattern $f(x, y)$

$$R(\rho, \varepsilon) = \int_{-\infty}^{\infty} \int_{-\infty}^{\infty} f(x, y) \delta(\rho - x \cos \varepsilon - y \sin \varepsilon) dx dy \quad (5)$$

which transform all points (x_i, y_i) on a Kikuchi line into a single point (ρ_i, ε_i) in Cartesian Hough space. ρ is the distance of the line from the origin, and ε is the angle between the perpendicular to the line at the origin and the x axis. The positions of bright and dark Kikuchi lines are then detected separately as bright peaks in a H^+ and cusps in a H^- Hough space, respectively.

Band profile analysis is performed, as an additional option, in the original pattern along a small strip enclosing the particular band. Since high-order lines rather than bands are a characteristic of TKP, corresponding line pairs are finally selected by considering the nearest pair of a bright and a dark peak as the lowest diffraction order of a band. Its spacing, the band width, yields the Bragg angle, and the center point between the peaks corresponds to the (imaginary) center line of the band. The so located bands are sorted according to their intensities and widths. Typically the 5 to 10 smallest and most intense bands are passed to the indexing routine. Allowance is made up to high-index bands, as a TKP consists of only a small angular section and a few zone axes, whilst consideration of the first 3 to 4 families of $\{hkl\}$ planes is usually sufficient for indexing a BKP due to its large angular range [7]. An example of automated indexing of a TKP is given in Figure 2. With lower crystal symmetry, bands and lines are becoming increasingly dense and overlaid. In these applications the interactive measurement of Kikuchi line positions (i.e. band positions *and* band widths) including the check of the results by the operator is still the more reliable technique.

The fully automated indexing of spot diffraction patterns has not yet been implemented since we have used SAD spot patterns only occasionally for interactive orientation measurement, as a consequence of the significantly inferior accuracy and spatial resolution as compared to Kikuchi patterns. A routine for extracting spot positions from the pattern is straight forward. A Hough transform is not needed. However, the (relative) spot intensities have to be taken into account as well, in addition to the spot positions, in order to improve the accuracy of obtained orientations. The center of a ring of bright spots rather than the primary beam spot marks the real position of the low indexed zone axis of these spots in the pattern. In order to exclude the 180° ambiguity, spots from different zones are highly desirable. A revival of orientation determination from spot diffraction patterns is expected from the availability of TEM with Köhler illumination systems and microbeam diffraction facility [8]. This technique allows the independent settings of primary beam aperture and spot diameter. A high spatial

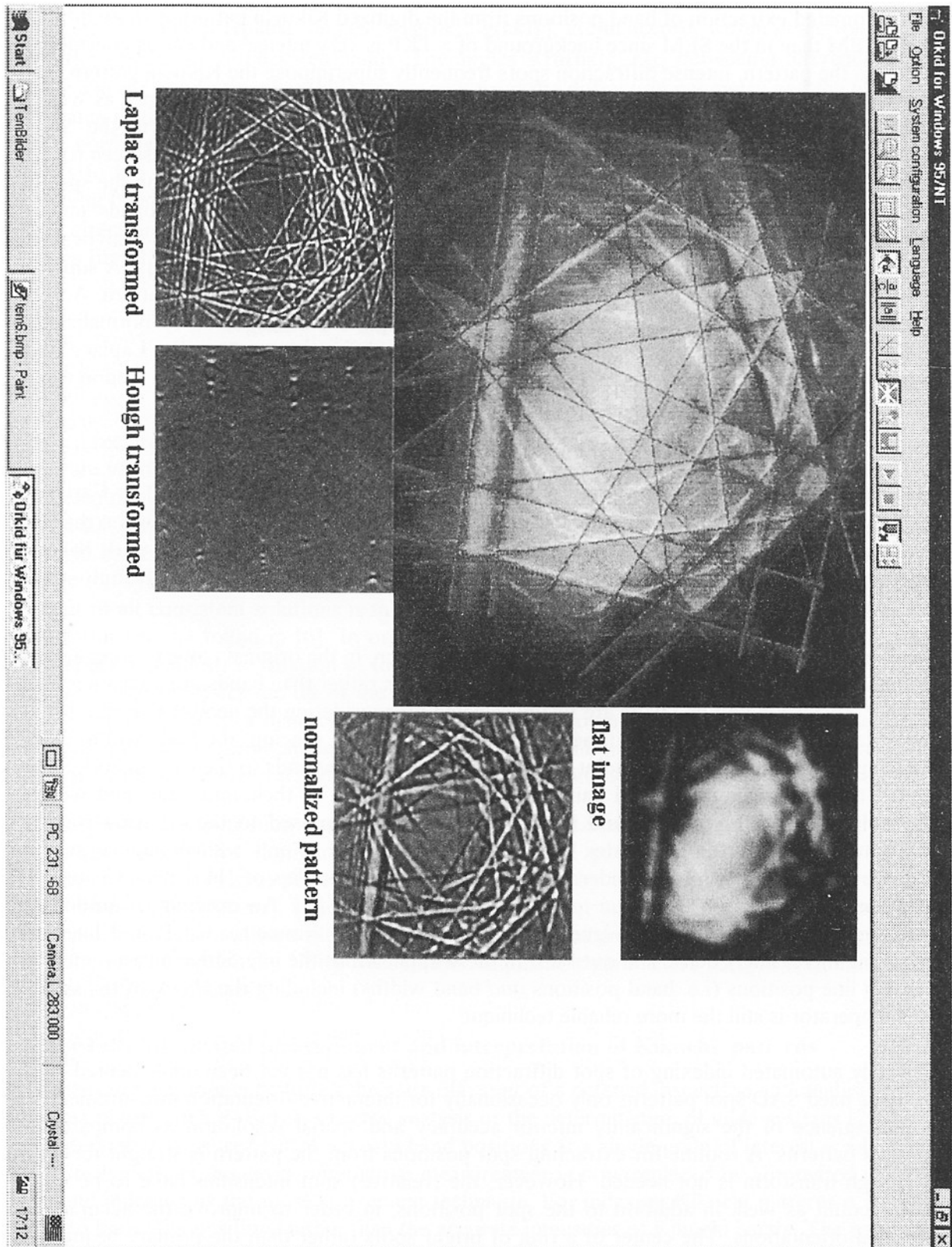


Figure 2 Automated indexing of a TKP

resolution, similar to the Kikuchi method, will be enabled since, with a fine though parallel beam, the diffraction spots remain sharp points in the pattern. Convergent beam electron diffraction (CBED) is sometimes used as a poor alternative. It suffers from the excessive widening of the diffraction spots, as a consequence of the increase in beam aperture when the beam diameter is decreased to focus on a grain of interest.

5. Automated crystal lattice orientation measurement and mapping

An ACOM system requires the automated translation of the beam spot across the stationary specimen in regular steps after each orientation measurement. In the PHILIPS EM 430 STEM the digital beam scanning signal from the computer is applied to the built-in pre-specimen deflection coils through a 12 Bit digital-to-analog converter. In order to avoid interference of low analog signals with electromagnetic hum, the digital-to-analog converter is placed in the hybrid diffraction unit rather than in the computer, and deflection signals are transmitted in digital form to the microscope. The primary beam spot as the pattern center stays virtually stationary during a parallel displacement of the primary beam across the specimen. The specimen need not be tilted for measurement. Hence no procedures for autocalibration of the pattern center nor dynamic focus control are required in the TEM, as contrasted to ACOM with digital beam scan in the SEM [7]. ACOM on the TEM is about three times slower (1 orientation per second) than on the SEM, due to the difficult background simulation, the software solution for contrast manipulation and the special treatment of superimposed diffraction spots and Kikuchi lines.

The grain orientation database from ACOM is used in supplementary programs for the calculation of the orientation distribution function (ODF), orientation correlation functions (MODF, nOCF, rOCF, higher-order correlations) and pole figures [9], or for a graphical representation of the microstructure by constructing Crystal Orientation Maps (COM) [10, 11]. Hereby the measured grid points are stained by colors specific for the crystal lattice orientations or misorientations across grain boundaries. Orientation parameters in COM may be the Euler angles ($\varphi_1, \Phi, \varphi_2$) or the Rodrigues vector \mathbf{R} . An orientation-to-color scale is defined by superimposing the basic colors red, green and blue with gradually increasing intensity on the axis of the Euler orientation space or Rodrigues orientation space, respectively. Allowance has to be made for equivalent subspaces when mixing the shaded colors to indicate oblique orientations. The disadvantage of Euler and Rodrigues space is an "umklapp" effect of colors: When the orientations approach the bordering planes of the Euler subspaces or when the Rodrigues vector jumps to another direction to account for a small rotation angle, a drastic change in color may appear although the change in orientation may only be infinitesimally small. Because of the easy way of interpretation and due to the continuous change of colors with continuously changing orientations we often prefer the representation by two crystallographic directions (hkl)[uvw] for two sample reference directions. The orientation triangle is superimposed by a color triangle with the red, green and blue colors in the [001], [011] and [111] corners, respectively, and the triangle is stained by running colors to make an orientation-to-color scale. Since the representation of a crystal lattice orientation requires *two* orientation triangles (one for each reference direction), two color maps are required in this case for the representation of the full spatial orientation distribution.

Misorientations can be calculated between successive image points, and grain boundaries or subboundaries can be marked as color lines by using a rotation-axis&rotation-angle representation, or – less precisely – by classifying the misorientations by the Σ notation of the CSL model on a linear scale. A grain boundary is characterized in detail, however, by the

combination of the misorientation of the abutting grains *and* the spatial orientation of the grain boundary normal. Grain boundary normals are obtained on-line, by switching the TEM to imaging mode, from the local foil thickness and the widths of the grain boundaries in the images at two angular tilts. This measurement is much simplified, if one of the images shows the grain boundary "edge-on". Since the misorientation is precisely known from individual grain orientation measurement, the grain boundary normal can be indexed with respect to either crystal lattice. In a similar way, other local properties or parameters can be represented graphically by color maps, such as dislocation density, the predominant glide systems or twin systems in the grains, the Schmid factor or the residual deformation energy in the individual grains [12].

A disadvantage of ACOM in the TEM is its sensitivity to irregular buckling of the thin foil. The lattice orientation may locally vary over the area of bending, and the microstructural orientation image will be superimposed by related orientation features giving rise to random or symmetrical patterns similar to bend contours in conventional bright or dark field images. These difficulties are much alleviated by using a high accelerating voltage which enables thicker specimens to be studied with the Kikuchi method.

ACKNOWLEDGMENT

Financial by the German Research foundation (DFG-Forschergruppe "Textur und Anisotropie kristalliner Stoffe") is gratefully acknowledged.

REFERENCES

- [1] R.A. Schwarzer: The study of crystal texture by electron diffraction on a grain-specific scale. *Microscopy and Analysis* **45**(1997), p. 35-37
- [2] R.A. Schwarzer and S. Zaefferer: Automated measurement of grain orientations and on-line determination of complete deformation systems with a TEM. *Adv. in X-Ray Analysis* **38**(1995), p. 377-381
- [3] H. Weiland and R.A. Schwarzer: On-line Auswertung von Kikuchi- und Channelling-Diagrammen. *Beitr. elektronenmikr. Direktabb. Oberfl. (BEDO)* **18**(1985), p. 55-60
- [4] S. Zaefferer and R.A. Schwarzer: Automated measurement of single grain orientations in the TEM. *Z. Metallkunde* **85**(1994), p. 585-591
- [5] H. Schumann: *Kristallgeometrie*, VEB-Verlag, Leipzig (1979)
- [6] R. Schwarzer: Die Bestimmung der lokalen Textur mit dem Elektronenmikroskop. Habilitation Thesis, TU Clausthal (1989)
- [7] R.A. Schwarzer: Automated crystal lattice orientation mapping using a computer-controlled SEM. *MICRON* **28**(1997), p. 249-265
- [8] G. Benner and W. Probst: Köhler illumination in the TEM: fundamentals and advantages. *J. Microscopy* **174**(1994), p.133-142
- [9] B. Schäfer: ODF computer program for individual orientation and pole figure data supporting all symmetries, arbitrary measuring ranges and calculation of material properties. *Materials Science Forum* **273-275**(1998), p. 113-118
- [10] D. Gerth and R.A. Schwarzer: Graphical representation of grain and hillock orientations in annealed Al-1% Si films. *Textures and Microstructures* **21**(1993), p. 177-193
- [11] F. Springer: Recent developments in Automated Crystal Orientation Mapping (ACOM) – Evaluation and graphical representation of individual grain orientation data. *Materials Science Forum* **273-275**(1998), p. 191-200
- [12] R.A. Schwarzer: Advances in crystal orientation mapping with the SEM and TEM. *Ultramicroscopy* **67**(1997), p. 19-24